

Phase Boundaries for Mixed Aqueous Micellar Solutions of Dimethyldodecylamine Oxide and Sodium or Magnesium Dodecyl Sulfate with Regard to Chemical Processes in the Systems

N. A. Smirnova,^{*,†} B. Murch,[‡] I. B. Pukinsky,[†] T. G. Churjusova,[†]
M. V. Alexeeva,[†] A. Yu. Vlasov,[†] and L. V. Mokrushina[†]

*St. Petersburg State University, Universitetsky pr.2, 198504 St. Petersburg, Russia, and
Procter & Gamble European Technical Center, Strombeek-Bever, Belgium*

Received October 3, 2001. In Final Form: January 25, 2002

The literature data bear witness to strong synergistic effects in mixed aqueous solutions of alkylamine oxides and alkyl sulfates. Physicochemical properties of these systems depend essentially on pH, which is due to protonation of amine oxide. Interplay of several types of intermolecular interactions including chemical ones results in complex phase diagrams. New experimental data presented in the paper refer to the solid–liquid equilibrium (the Krafft boundary), the composition of crystallizing complexes, and the critical micelle concentration (cmc) in mixed aqueous solutions containing dimethyldodecylamine oxide and sodium or magnesium dodecyl sulfate. The temperature maximum suggesting the formation of a 1:1 amine oxide–dodecyl sulfate complex is observed at the curves of dissolution temperature versus surfactant-based composition; the shape of the curves indicates that complexes of other stoichiometries can be formed in solutions enriched with amine oxide. The dissolution temperature for the 1:1 mixture (and correspondingly, the concentration of the complex in the solution) grows with growing acidity. In both systems under study, the dissolution temperature becomes 48 °C at a pH of about 5 and does not change on further pH lowering. Chemical analysis has shown that the solid phase precipitated from basic solutions contains metal ions whereas at pH ≤ 5 the complex between the protonated amine oxide and dodecyl sulfate anion is crystallized. The cmc value for 1:1 acidic mixtures does not depend on the cation nature and is 2 orders of magnitude lower than that for solutions at the natural pH (which are slightly basic). The pseudophase model taking into account the reactions of amine oxide protonation and 1:1 complex formation reproduces satisfactorily the pH effect on the solubility diagrams in the dimethyldodecylamine oxide–sodium dodecyl sulfate–water system.

1. Introduction

Aqueous mixtures of alkylamine oxides and dodecyl sulfates draw much attention owing to their peculiar physicochemical behavior and miscellaneous applications. Various data, in particular those on concentration dependence of the surface tension, critical micelle concentration (cmc), Krafft temperature, pH, viscosity, foaming, solubilization, and so forth^{1–10} give evidence of strong synergistic effects on addition of anionic surfactants to alkylamine oxides which are classified as semipolar

surfactants. Interplay of several types of intermolecular interactions including chemical ones results in complex phase diagrams for the systems of interest. Among other properties, the phase boundaries for the micellar region in ternary systems amine oxide–anionic surfactant–water are of substantial interest. In the present study, primary attention is paid to the dissolution temperature–composition diagram (the Krafft boundary) for mixed micellar solutions containing dimethyldodecylamine oxide (C₁₂AO, AO) and sodium or magnesium dodecyl sulfate (NaDS or Mg(DS)₂), the dependence of the temperature on the overall and relative concentration of the surfactants and on pH, the composition of the solid phases crystallized from various mixtures, and thermodynamic approaches to description and prediction of the phase behavior. Specificity of the dissolution temperature versus surfactant-based composition dependence for the C₁₂AO–NaDS–H₂O system was marked in ref 11. The authors report that the solubility curve exhibits two eutectic-looking minima and an interstitial maximum at C_nAO/NaDS = 3:1 (n = 12, 14) giving evidence of complex formation. However, the solubility diagram was studied only at natural pH. The data on the phase behavior for mixtures of amine oxide with magnesium dodecyl sulfate are missing in the literature. The effect of pH upon the solubility diagrams was not investigated for the mixed micellar systems mentioned above or for any similar surfactant mixtures.

* Corresponding author. E-mail: smirnova@nonel.pu.ru.

[†] St. Petersburg State University.

[‡] Procter & Gamble European Technical Center.

(1) Weers, J. G.; Rathman, J. F.; Scheuing, D. R. *Colloid Polym. Sci.* **1990**, *268*, 832–846.

(2) Kakitani, M.; Imae, T.; Furusaka, M. *J. Phys. Chem.* **1995**, *99*, 16018–16023.

(3) Pils, H.; Hoffmann, H.; Hofmann, S.; Kalus, J.; Kencono, A. W.; Lindner, P.; Ulbricht, W. *J. Phys. Chem.* **1993**, *97*, 2745–2754.

(4) Bakshi, M. S.; Crisantino, R.; De Lisi, R.; Milioto, S. *J. Phys. Chem.* **1993**, *97*, 6914–6919.

(5) Hofmann, S.; Rauscher, A.; Hoffmann, H. *Ber. Bunsen-Ges. Phys. Chem.* **1991**, *95*, 153–164.

(6) Hoffmann, H. In *Structure and Flow in Surfactant Solution*; Herb, C. A., Prud'homme, R. K., Eds.; ACS Symposium Series 578; American Chemical Society: Washington, DC, 1994; pp 2–31.

(7) Hoffmann, H. In *Organized Solutions*; Friberg, S. E., Lindman, B., Eds.; Surfactant Science Series Vol. 44; Marcel Dekker: New York, 1992; pp 169–192.

(8) Hoffmann, H.; Hofmann, S.; Illner, J. C. *Prog. Colloid Polym. Sci.* **1994**, *97*, 103–109.

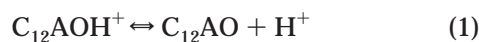
(9) Maeda, H.; Kakehashi, R. *Adv. Colloid Interface Sci.* **2000**, *88*, 275–293.

(10) Rosen, M. J.; Friedman, D.; Gross, M. *J. Phys. Chem.* **1964**, *68*, 3219–3225.

(11) Tsujii, K.; Okahashi, K.; Takeuchi, T. *J. Phys. Chem.* **1982**, *86*, 1437–1441.

2. Overview of Studies on Aggregation and Chemical and Phase Behavior of Aqueous Mixtures of C_nAO and NaDS

The properties of solutions containing an amine oxide are affected by the following peculiarity of its headgroup: the N—O bond has a pronounced dipole moment equaling 4.38 D.¹² The excessive electron charge localized on the O atom makes it a proton acceptor capable of formation of strong hydrogen bonds.¹³ On the other hand, this excessive charge predetermines the amphoteric character of the surfactant that can exist in nonionic and cationic forms. In the case of C₁₂AO, the equilibrium between these moieties can be described as



$$K_a = \frac{a_{\text{C}_{12}\text{AO}} a_{\text{H}^+}}{a_{\text{C}_{12}\text{AOH}^+}} \quad (2)$$

where K_a is the dissociation constant, a_i is the activity of species i ($i = \text{C}_{12}\text{AO}, \text{C}_{12}\text{AOH}^+, \text{H}^+$). The definition in eq 2 gives the true thermodynamic equilibrium constant, which is independent of the surfactant concentration and pH. If the relevant choice of the reference state is made, the activities $a_{\text{C}_{12}\text{AO}}$ and $a_{\text{C}_{12}\text{AOH}^+}$ can be equalized with the molar concentrations of the corresponding species in highly diluted solutions. The apparent dissociation constant K_{app} can be introduced as

$$K_{\text{app}} = \frac{C_{\text{C}_{12}\text{AO}} a_{\text{H}^+}}{C_{\text{C}_{12}\text{AOH}^+}} \quad (3)$$

This quantity is concentration dependent and becomes equal to K_a at high dilutions.

As stems from eq 1, in the basic media amine oxide will behave as a typical nonionic surfactant, and in the acidic solutions it will manifest the properties of a cationic one. According to the literature data, aliphatic amine oxides are weak bases with characteristics close to those of the acetate ion. Like other amphoteric containing weak groups, amine oxides show considerable buffering in distinction to strong acids or strong base surfactants.

Estimation of equilibrium constants in highly diluted solutions (below the cmc) does not encounter any specificity compared to reactions occurring in typical solutions of weak electrolytes. However, in describing chemical equilibria in the concentration range beyond the cmc one should take into account that the protonation degree of amine oxide in micelles and in the aqueous medium is not the same. Nonideal behavior of the mixture of protonated and neutral forms of amine oxide in micelles is a problem of great concern. The established negative deviation from ideality is ascribed to the electrostatic effect: the Coulomb repulsion among positively charged headgroups tends to diminish when they are mixed with neutral ones.^{14,15} Association by hydrogen bonding may also exert a considerable effect on equilibrium characteristics of the protonation reaction.^{16,17}

(12) Lake, D. B.; Hoh, G. L. K. *J. Am. Oil Chem. Soc.* **1963**, *40*, 628–631.

(13) Oswald, A. A.; Guertin, D. L. *J. Org. Chem.* **1963**, *28*, 651–657.

(14) Tokiwa, F.; Ohki, K. *J. Phys. Chem.* **1966**, *70*, 3437–3441.

(15) Rathman, J. F.; Christian, S. D. *Langmuir* **1990**, *6*, 391–395.

(16) Maeda, H.; Muroi, S.; Ishii, M.; Kakehashi, R.; Kaimoto, H.; Nakahara, T.; Motomura, K. *J. Colloid Interface Sci.* **1995**, *175*, 497–505.

(17) Maeda, H. *Colloids Surf., A* **1996**, *109*, 263–271.

In refs 14–17, two apparent protonation constants dependent on pH are viewed: those for monomers and micelles. The value of pK_{app} for the monomer form (4.8–5.0 at 25 °C, concentrations C in eq 3 being in mol/dm³) is lower than that for the micelles (5.6–6.0), both increasing linearly with the salt concentration.¹⁶ Rathman and Christian¹⁵ in the frame of the pseudophase model have shown that the constant K_a expressed through the activities of protonated and neutral amine oxide in micelles is approximately equal to the apparent concentration constant K_{app} for monomer forms.

The amphoteric character of C_nAO is responsible for the pronounced dependence of micellization characteristics on pH, the cmc versus pH curves exhibiting a minimum.^{14,15,17} The shape of micelles and their sizes are also affected by the acidity of the solution.^{2,3,18–20} The domination of nonprotonated moieties at high pH favors the enlargement of aggregates.

The phase diagrams of the C₁₂AO–H₂O and C₁₂AO–HCl–H₂O systems were investigated on the basis of small-angle X-ray diffraction, NMR, polarized light microscopy, and differential scanning calorimetry (DSC).^{21–24} The solid-state phase behavior of C₁₂AO was studied and interpreted with regard to protonation and counterion effects in ref 25. The phase diagram of the C₁₄AO–H₂O system was considered in ref 26. The lower temperature boundary for the micellar solutions in the C₁₂AO–H₂O and C₁₄AO–H₂O systems is determined by ice formation (approximately 0 °C).

In the ternary systems C_nAO–NaDS (Mg(DS)₂)–H₂O, protonated amine oxide turns out to be involved in several types of rather strong bonding interactions of its headgroup with that of the anionic surfactant. They are electrostatic ion–ion interactions, ion–dipole interactions, and hydrogen bonding. Ion–ion electrostatic interactions pertain to the straight interaction of the protonated form of amine oxide with the negatively charged dodecyl sulfate ions. This type of interaction is typical for anionic/cationic surfactant mixtures²⁷ and may result in formation of a 1:1 complex. Strong ion–dipole interactions are due to the aforementioned dipole moment of the NO-group in amine oxide. They occur between the positive portion of the dipole (centered on N) and the negatively charged sulfate ion. The structure which results from this interaction is somewhat analogous to that of a double-tail anionic surfactant. The ion–dipole interactions bring the AO and DS[−] moieties in close proximity, which leads to an excessive crowding of the methylene tails, as is detected in spectra for the CH-stretching region.¹ The large reduction of the effective headgroup area provokes formation of rodlike micelles. Similar effects can be caused by hydrogen-bonding interactions of hydrated headgroups

(18) Ikeda, S.; Tsunoda, M.-A.; Maeda, H. *J. Colloid Interface Sci.* **1979**, *70*, 448–455.

(19) Herrmann, K. W. *J. Phys. Chem.* **1962**, *66*, 295–300; **1964**, *68*, 1540–1546.

(20) Kaimoto, H.; Shoho, K.; Sasaki, S.; Maeda, H. *J. Phys. Chem.* **1994**, *98*, 10243–10248.

(21) Lutton, E. S. *J. Am. Chem. Soc.* **1966**, *43*, 28–30.

(22) Lawson, K. D.; Mabis, A. J.; Flautt, T. J. *J. Phys. Chem.* **1968**, *72*, 2058–2065.

(23) Lawson, K. D.; Flautt, T. J. *J. Phys. Chem.* **1968**, *72*, 2066–2074.

(24) Fukada, K.; Kawasaki, M.; Kato, T.; Maeda, H. *Langmuir* **2000**, *16*, 2495–2501.

(25) Kawasaki, H.; Fukuda, T.; Yamamoto, A.; Fukada, K.; Maeda, H. *Colloids Surf., A* **2000**, *169*, 117–124.

(26) Hoffmann, H.; Oetter, G.; Schwandner, B. *Prog. Colloid Polym. Sci.* **1987**, *73*, 95–106.

(27) Holland, P. M.; Rubingh, D. N. *Mixed Surfactant Systems*; Holland, P. M., Rubingh, D. N., Eds.; ACS Symposium Series 501; American Chemical Society: Washington, DC, 1992; pp 2–30.

of the surfactants. Ion–dipole interactions and hydrogen bonding may determine formation of complexes with various stoichiometries, not solely 1:1 (contrary to the case of the ion–ion interactions).

The complex character of interparticle interactions predetermines peculiar structural and thermodynamic properties of the ternary micellar solutions under discussion, such as nonlinear dependence of pH, cmc, surface and interfacial tension versus mixing ratio of surfactants, strong synergistic effects manifested through a high tendency to self-ordering in the mixture, a sophisticated topology of the phase diagram, and so forth.

Contrary to the C_n AO–cationic surfactant systems displaying linear dependence of their natural pH on mixing ratio, solutions formed by C_n AO and anionic surfactants exhibit a pH maximum.¹ The equimolar mixture of C_{12} AO and NaDS with the overall content of the surfactants being 40 mM at 25 °C has a pH of about 10, whereas pH values of solutions of each of the individual surfactants do not exceed 8. Even small amounts of NaDS added to C_{12} AO or C_{14} AO solutions shift pH considerably to higher values. Negative deviations from the ideal behavior are appropriate to the composition dependence of the cmc and the partial molar volume.⁴ Drastic changes in the rheological behavior of the systems were registered in some composition intervals, viscoelastic properties being observed.^{1,5}

The nonlinear concentration dependence of the aggregation number and pH starts from the electrostatic coupling between the protonated amine oxide and DS^- ions.² Evidently, the coupling causes a displacement of the amine oxide protonation equilibrium expressed by eq 1 to the left side, and this is followed by a release of hydroxyl ions and by an increase in pH.

As is mentioned above, the solubility diagrams for ternary systems C_n AO–NaDS– H_2O ($n = 12, 14$) are discussed in ref 11. Mixtures with the overall content of the surfactants being 100 mM were studied at natural pH. The diagrams are not presented in the paper, but it is reported that the addition compound between the anionic surfactant and protonated amine oxide is formed. The composition of the compound is determined as C_n AO/NaDS equaling 3:1; the Krafft temperatures are around 26 and 17.5 °C for $n = 12$ and 14, respectively; in the latter case the differential heat of dissolution of 26 kJ mol⁻¹ is given.

In the present work, the temperatures of the micellar solution–solid phase equilibrium were determined in the systems NaDS– H_2O , Mg(DS)₂– H_2O , C_{12} AO–NaDS– H_2O , and C_{12} AO–Mg(DS)₂– H_2O over a wide range of surfactant/water and amine oxide/sulfate mole ratios (in the ternary systems). Rather concentrated mixed micellar solutions were under study (whereas most of the literature data on the dissolution temperature in mixed systems relate to surfactant concentrations not much higher than the cmc). The solubility diagrams in the systems containing amine oxide have been investigated at various pH values. The effects of pH on the solubility diagram in mixtures of anionic and semipolar surfactants were not studied until now, and our goal was both to get experimental data and to model the observed behavior with regard to chemical processes in the system.

3. Experimental Section

3.1. Materials. NaDS (>99% purity) was obtained from Fluka Co. Ltd. C_{12} AO was delivered by Hoechst Co. (Gendorf, Germany) as a 29.8 wt % solution. The surfactants were used without further purification. Mg(DS)₂ was precipitated from an aqueous solution of NaDS and MgCl₂ with a molar ratio of 2:1 by slow cooling of the solution down to a temperature of 22–23 °C. The conditions

of precipitation were chosen taking into account the characteristics of the dissolution diagram in the system NaDS–MgCl₂– H_2O . The obtained crystals of Mg(DS)₂ were separated by filtration, and then the sample was recrystallized twice from distilled water and was dried until attaining a constant mass. The purity of the product was examined by complexometric titration with the disodium salt of ethylenediaminetetraacetic acid (EDTA) and turned out to be 98%. Samples of crystal hydrate MgCl₂·6 H_2O used in the work were of analytical grade. All of the solutions were prepared using distilled or bidistilled water free of CO₂.

3.2. Experimental Procedures. The study of the micellar solution–solid phase equilibrium was performed mostly by visual observations of the dissolution temperature when the investigated heterogeneous mixture was slowly heated. In our experiments, the samples were equilibrated at temperatures below that of surfactant dissolution but higher (at least slightly) than that of ice crystallization. The samples were prepared according to the following procedure. The mixture (about 2 mL) made by weighing was placed into a hermetically closed vessel or was sealed in an ampule (the last procedure was applied to solutions with pH > 7 to prevent absorption of CO₂ during their long storage). The sample was stored at 0 °C until the solid phase appeared. After that, the two-phase mixture was kept for several days more to accomplish the process of crystallization. Special care should be paid to receive a stable solid crystal phase, and in some cases more than a month was needed for this. In particular, mixed basic solutions of C_{12} AO and NaDS at 0 °C can exist for a long time in a metastable liquid state. When the temperature of such metastable mixtures is decreased down to –1 °C, crystals of pure ice easily appear, instead of the stable solid phase composed of surfactants.

After the liquid solution–solid crystal equilibrium was attained, the vessel (ampule) containing the two-phase system was inserted into a glass container connected to a thermostat. Then the heterogeneous sample was heated gradually; a magnetic stirrer was used. We stepped the temperature up by 2–3 °C at the beginning and by 0.2–0.3 °C when approaching the dissolution temperature. In the vicinity of the dissolution temperature, the sample was kept at each step at least for 20–30 min to ensure that equilibrium was established. The dissolution temperature was estimated as an average of two temperature values: the lower one was for the liquid system containing traces of the solid phase, and the upper one was for the homogeneous solution.

In the acidic medium (pH ≤ 5.5), some solutions were not transparent and the conventional visual method could not be applied. In this case, the dissolution temperature was measured using a polarized light microscope (Reichert, Austria) equipped with a heating stage.

For each sample, measurements were repeated several days (sometimes weeks) later until a stable value of the dissolution temperature was obtained.

The mean error in experimentally determined dissolution temperatures is 0.3 °C for solutions of individual surfactants and 1 °C for surfactant mixtures.

Calorimetric measurements of the temperatures and enthalpies of phase transitions were carried out for the precipitates with a differential scanning calorimeter (DSC-111, Setaram) at a heating rate of 1 °C min⁻¹.

All pH measurements were performed at a temperature of 50 °C (in the absence of the solid phase) using the pH-150 pH meter with a glass electrode and a silver/silver chloride reference electrode.

X-ray powder diffraction was measured by an X-ray diffractometer (DRON 2.0, Russia), with graphite-monochromated Cu Kα1 radiation being used. The scan speed and step size for 2θ were 2° min⁻¹ and 0.1°, respectively.

The analytical procedure applied to determine the composition of precipitated solid samples is described in part 4.3.

The cmc values in aqueous solutions of NaDS, Mg_{1/2}DS, C_{12} AO, and their mixtures have been measured using the dodecyl sulfate selective electrode and by the contact angle technique. The experimental procedure is described elsewhere.²⁸

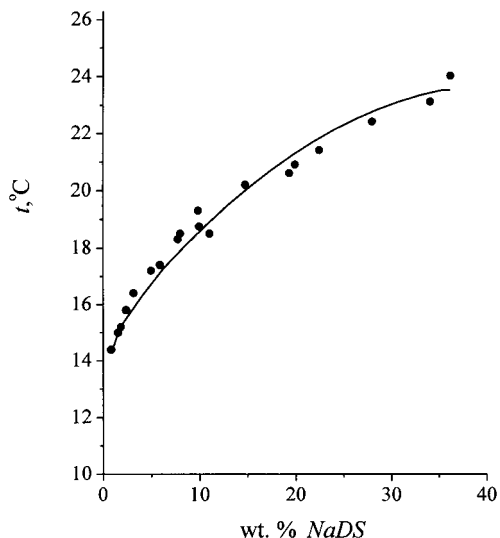


Figure 1. The dissolution temperature versus the concentration in the NaDS–H₂O system.

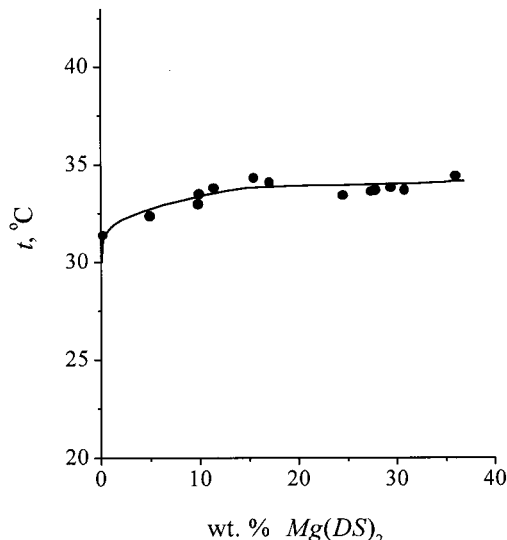


Figure 2. The dissolution temperature versus the concentration in the Mg(DS)₂–H₂O system.

4. Results and Discussion

4.1. Solubility Diagrams for Individual Surfactants. C₁₂AO–H₂O. The measurements have shown that micellar solutions in this system undergo ice crystallization on cooling, and therefore the lower temperature boundary for the solutions is around 0 °C (a bit lower than 0 °C).

NaDS–H₂O. The temperature of surfactant dissolution was measured in the range of concentration of micellar solutions from 0.87 to 36.2 wt % of NaDS (Figure 1). Our data are in good agreement with those from the literature.^{29–31} According to the literature data, the dihydrate of NaDS is crystallized from the micellar solutions. The reported temperature for the Krafft point is 9 °C,³² and cmc = 8.1–8.3 mM at 25 °C.^{32,33}

Mg(DS)₂–H₂O. The Krafft boundary was determined in the concentration range from 0.2 to 36 wt % of the surfactant (Figure 2). The growth of the dissolution temperature along this part of the boundary comprises about 3 °C. In accord with ref 34, the allocation of the Krafft point for Mg_{1/2}DS is $t = 25$ °C, and cmc = 1.8 mM.

4.2. Solubility Diagrams for Aqueous Mixtures of Two Surfactants at Various Acidities. The following composition variables are used below:

$$x'_{AO} = \frac{x_{AO}}{x_{AO} + x_{MeDS}} \quad x'_{HCl} = \frac{x_{HCl}}{x_{HCl} + x_{AO}}$$

$$x_{total} = x_{AO} + x_{MeDS}$$

where x_i is the mole fraction of component i in the mixture; Me = Na, Mg_{1/2} (the concentration of magnesium dodecyl sulfate is given in gram-equivalents, that is, related to Mg_{1/2}DS).

(28) Alexeeva, M. V.; Bart, T. Ja.; Morachevski, A. G.; Smirnova, N. A. *Vestnik St. Petersburg Univ.* **1999**, Ser. 4, Issue 3, 54–59.

(29) Laughlin, R. G. *The aqueous phase behavior of surfactants*; Academic Press: New York, 1994; Chapter 5.

(30) Kekicheff, P.; Grabielle-Madellmont, C.; Ollivon, M. *J. Colloid Interface Sci.* **1989**, 131, 112–132.

(31) Kogan, V. B.; Fridman, V. M.; Kafarov, V. V. *Spravochnik po rastvorimosti (Handbook on Solubility)*; Akad. Nauk SSSR: Moscow-Leningrad, 1961; Vol. 1, p 145.

(32) Hato, M.; Shinoda, K. *J. Phys. Chem.* **1973**, 77, 378–381.

(33) Markina, Z. N.; Panicheva, L. P.; Zadymova, N. M. *Colloid J.* **1996**, 58, 795–801 (in Russian).

(34) Hato, M.; Tahara, M.; Suda, Y. *J. Colloid Interface Sci.* **1979**, 72, 458–464.

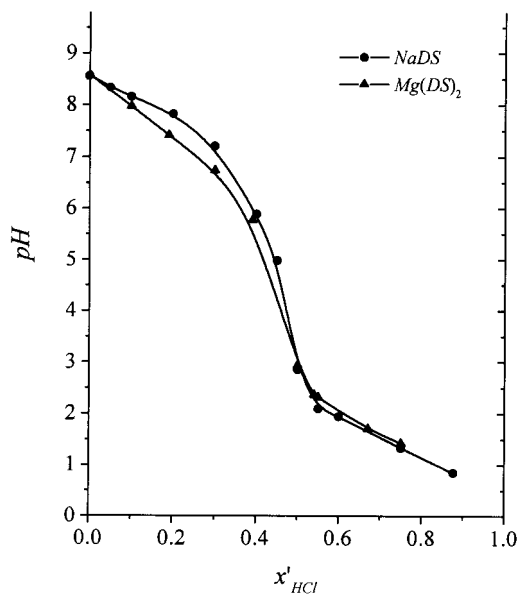


Figure 3. Dependence of pH on x'_{HCl} for C₁₂AO–NaDS–HCl–H₂O and C₁₂AO–Mg(DS)₂–HCl–H₂O solutions at $x_{AO} = x_{MeDS} = 0.0005$ and $t = 50$ °C.

The solid–liquid phase equilibrium was studied along the cross section of the composition triangle $x_{total} = 0.001$ (0.1 mol %) and in addition for the overall surfactant content equal to 10 wt %. Measurements were performed at natural values of pH and for more acidic mixtures. The dependence of the dissolution temperature on x'_{AO} was studied at a fixed value of x'_{HCl} . The relationship between the latter and the pH value for mixtures at $x_{AO} = x_{MeDS} = 0.0005$ and 50 °C is shown in Figure 3.

C₁₂AO–NaDS–H₂O. Experimental results are presented in Figures 4–6. The left branch of the solubility diagram (Figure 4) at a given pH corresponds to solutions from which NaDS crystallizes. This branch intersects with the line of crystallization of the ice (at natural pH) or (in more acidic mixtures) with the curve of crystallization of the compound formed by amine oxide and dodecyl sulfate. As is seen, the change in the acidity does not affect substantially the slope of the branch of NaDS crystallization, but the whole diagram changes drastically. Its topology witnesses that in the acidic mixtures over a wide range of middle concentrations the complex AO/DS = 1:1

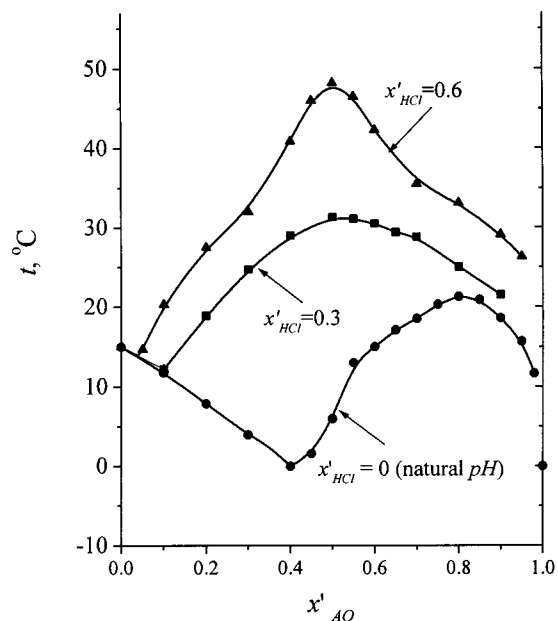


Figure 4. The dissolution temperature versus x'_{AO} in the C_{12} -AO-NaDS-HCl- H_2O system at $x_{total} = 0.001$.

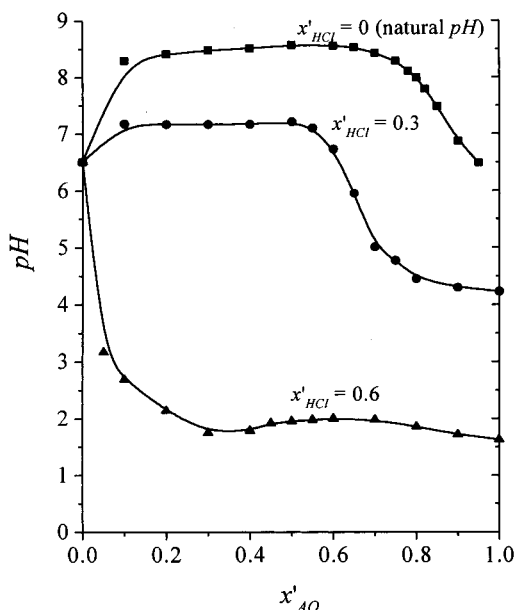


Figure 5. The dependence of the pH value on x'_{AO} in the C_{12} -AO-NaDS-HCl- H_2O solutions at $x_{total} = 0.001$.

is crystallized. The diagrams show that compounds with other stoichiometries (presumably AO/DS = 4:1) can exist, at least at natural pH. From solutions with a high content of amine oxide, ice is crystallized (the corresponding horizontal line at 0 °C is very short).

The value of the dissolution temperature observed at AO/DS = 1:1 grows when pH goes down to pH = 3–4. It is seen in Figure 6 that the growth has a limit, viz., 48.2 °C attained at $x'_{HCl} = 0.5$. At $x'_{AO} = 0.8$, the dissolution temperature also increases with increasing acidity of the solution, which gives evidence that both compounds are formed with participation of protonated amine oxide. On addition of the acid, the concentration of the protonated form grows which causes the increase of the compound concentration and the growth of the dissolution temperature. In the basic medium, where the protonation reaction is suppressed, formation of the 4:1 compound is not

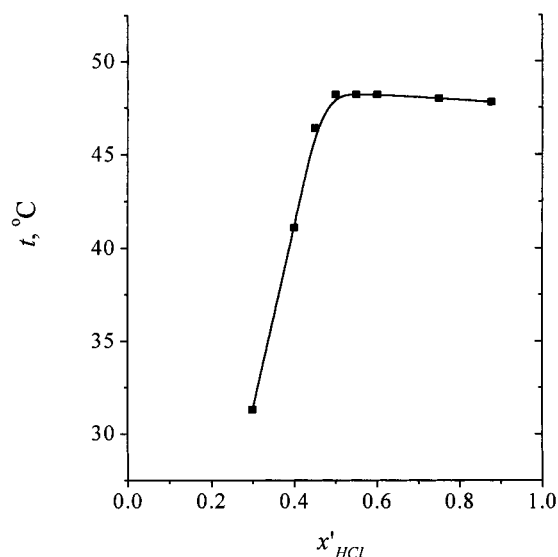


Figure 6. The dissolution temperature as a function of x'_{HCl} in the C_{12} AO-NaDS-HCl- H_2O system at $x_{AO} = x_{NaDS} = 0.0005$.

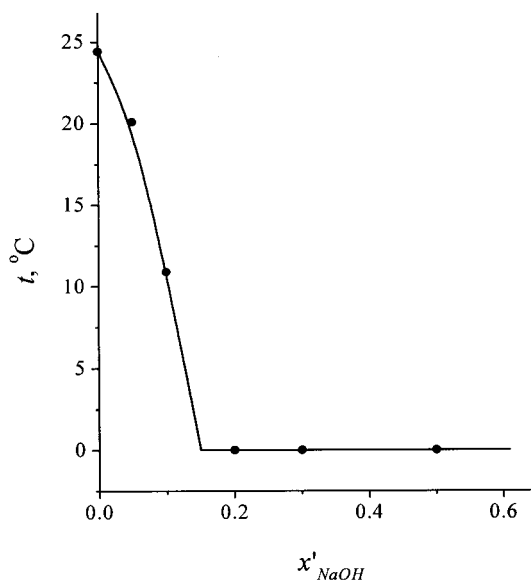


Figure 7. The dissolution temperatures as a function of x'_{NaOH} in the C_{12} AO-NaDS-NaOH- H_2O system at $x'_{AO} = 0.8$ and $x_{total} = 0.001$; $x'_{NaOH} = x_{NaOH}/(x_{AO} + x_{NaOH})$.

observed; at $x'_{AO} = 0.8$ precipitation from solutions with added NaOH starts around 0 °C (Figure 7).

$C_{12}AO-Mg(DS)_2-H_2O$. The data on dissolution temperatures at various surfactant concentrations and pH values are presented in Figures 8–10. The topology of the solubility diagrams is similar to that for $C_{12}AO$ -NaDS mixtures, but formation of the 1:1 compound between $C_{12}AO$ and $Mg_{1/2}DS$ is well pronounced already at natural pH. The “shoulder” in the range $x'_{AO} \geq 0.6$ suggests that not only 1:1 compound is formed.

Figure 10 presents the dissolution temperature against the amount of added HCl at an equimolar ratio of $C_{12}AO$ and $Mg_{1/2}DS$. It is seen that with the increase of x'_{HCl} the dissolution temperature at first decreases, then goes up, and at last ($x'_{HCl} > 0.55$) takes nearly the constant value of 48.5 °C.

4.3. Separation and Study of Solid Phases. Samples of the solid phases formed in aqueous mixtures AO/MeDS = 1:1 (Me = Na, $Mg_{1/2}$) at various pHs were separated. The mixtures under study are enumerated in Table 1.

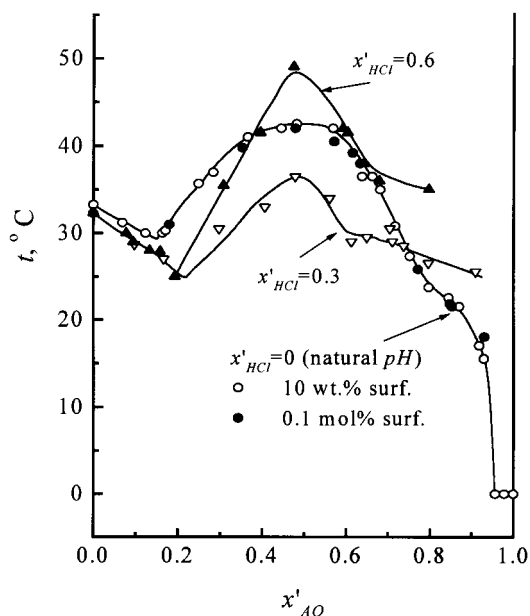


Figure 8. The dissolution temperature versus x'_{AO} in the $C_{12}AO-Mg(DS)_2-HCl-H_2O$ system at various pHs; the total surfactant content is 0.1 mol % (0.1 mol %, 10 wt % at natural pH).

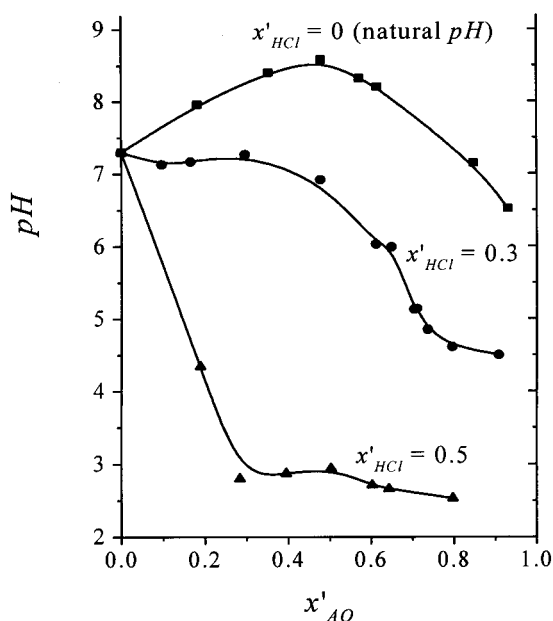


Figure 9. The dependence of the pH value on x'_{AO} in the $C_{12}AO-Mg(DS)_2-HCl-H_2O$ solutions of various acidity, $x_{total} = 0.001$.

The investigated heterogeneous mixture prepared by weighing was heated, and the solid phase was dissolved. The obtained homogeneous solution was filtered, slowly cooled to a temperature which was 6–7 °C lower than the dissolution temperature, and then kept at constant temperature for several days (deeper cooling was avoided as in this case not only the solid phase, which is in equilibrium with the saturated solution under study, but also other compounds could crystallize). The deposited crystals were separated from the liquid and dried in an evacuated vessel containing $CaCl_2$.

The results of the chemical analysis presented in Table 2 show that the content of magnesium in precipitates I–IV decreases with increasing acidity of solutions and at x'_{HCl} beyond 0.4 (pH \leq 5) only its traces are registered. The

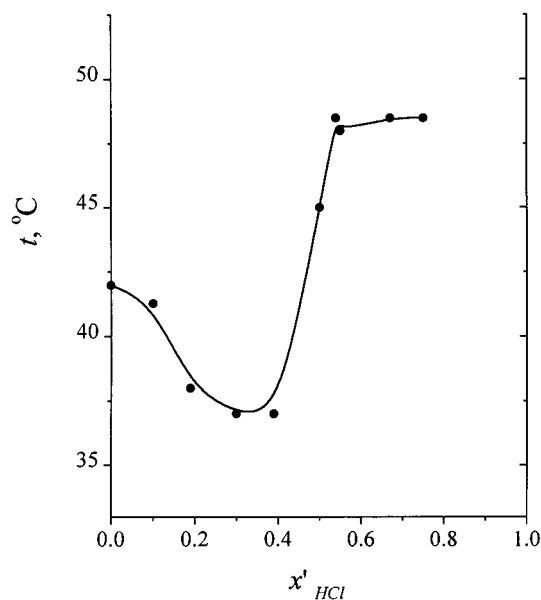


Figure 10. The dissolution temperature as a function of x'_{HCl} in the $C_{12}AO-Mg(DS)_2-HCl-H_2O$ system at $x_{AO} = x_{Mg_{1/2}DS} = 0.0005$.

Table 1

mixture	solid phase	x'_{HCl}	pH
$C_{12}AO-Mg_{1/2}DS-HCl-H_2O$	I	0	8.5
	II	0.33	6.3
	III	0.42	4.8
	IV	0.60	2.0
$C_{12}AO-NaDS-HCl-H_2O$	V	0.60	2.0

Table 2. Results of the Chemical Analysis of the Solid Phase Samples

element	wt %					calculated for AOH^+DS^- complex
	I	II	III	IV	V	
C ^a	54.2	59.4	62.0	62.7	63.5	63.0
H ^a	10.2	10.7	11.3	11.4	11.7	11.6
N ^a	2.1	2.5	2.6	2.6	2.6	2.8
Mg ^b	2.2	0.9	0.2	Mg in traces		
Na ^c	Na in traces					

^a Burning. ^b Complexometric titration with EDTA. ^c Emission spectroscopy.

solid phases deposited at pH = 2 in system IV (with $Mg_{1/2}DS$) and system V (with $NaDS$) are practically identical; their composition corresponds to that of the AOH^+DS^- complex.

The likeness of the structures of samples IV and V is confirmed by X-ray diffraction experiments; the powder diffraction patterns are given in Figure 11.

Similar results were obtained in the DSC measurements. The DSC thermograms for crystal samples IV and V are quite similar and differ from those for samples I–III. For samples IV and V, three phase transitions were observed in the DSC patterns. They correspond, from the low-temperature side, to the transition between solid 1 and solid 2 ($t = 62$ °C, $\Delta H = 62.8$ J/g), the melting of solid 2 to the liquid crystal (LC) ($t = 92$ °C), and the transition from the LC phase to the isotropic liquid ($t = 97$ °C). This phase sequence was confirmed by observation in polarized light. Only two phase transitions were observed for the nonionic species (sample I). They correspond to the transition between a solid and the LC phase ($t = 65.8$ °C, $\Delta H = 167.0$ J/g) and to that from LC to an isotropic liquid ($t > 110$ °C).

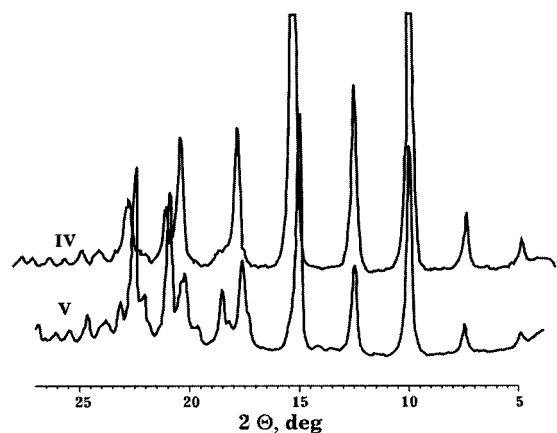


Figure 11. Powder diffraction patterns of crystals IV and V.

Table 3. Critical Micelle Concentration [mM] for Aqueous Solutions of the Individual Surfactants and Their Equimolar Mixtures, $t = 50\text{ }^{\circ}\text{C}$

pH	NaDS	Mg _{1/2} DS	C ₁₂ AO ^a	C ₁₂ AO–NaDS	C ₁₂ AO–Mg _{1/2} DS
natural	9.5	1.4	1.6	0.65	0.25
2				0.003	0.003

^a Measured by the contact angle technique at room temperature.

Thus, the study performed by various techniques gives evidence that the composition and structure of solid phases IV and V are identical, with these phases presenting crystals of the AOH⁺DS⁻ compound.

4.4. Critical Micelle Concentration. The results of the cmc measurements performed at 50 °C by the potentiometry method (using a dodecyl sulfate selective electrode) and by the contact angle technique are presented in Table 3. The cmc values obtained for aqueous solutions of NaDS, Mg(DS)₂, and C₁₂AO agree well with the literature data (the latter relate to other temperatures, but the temperature dependence of the cmc is not great). The data obtained for mixed solutions of amine oxide and sodium (magnesium) dodecyl sulfate show the drastic effect of acidity on the cmc value in these mixtures. As is seen for the acidic mixtures (pH = 2), the cmc value is 2 orders of magnitude lower than at the natural pH (~8) and it does not depend on the cation nature. This cmc value is of the same order as that for nonionic surfactants with a double hydrophobic tail.

It would be of great interest to investigate the structure of aggregates forming at cmc.

5. Thermodynamic Modeling of Solid–Liquid Equilibria in the Ternary System C₁₂AO–NaDS–H₂O

Strong synergistic effects depending on pH and a sophisticated topology of phase diagrams are peculiarities of the C₁₂AO–NaDS–H₂O system. The shape of the solubility diagram indicates that the two surfactants form additional compounds. The temperature maximum relating to the formation of the 1:1 complex is distinctly pronounced, especially at lower pH. The growth of the maximum temperature with growing acidity (down to pH = 3) is the indication of the increasing concentration of the complex. For the sake of simplicity in modeling the pH effect on the solid–liquid equilibrium, we confine ourselves to considering solely the 1:1 compound. Possibilities of formation of other compounds in mixtures enriched in amine oxide will not be discussed herein. Consequently, we view only the range of concentrations from pure NaDS to its surfactant-based mole fraction 0.5.

The first model consideration of the system under study was proposed in ref 35. A modified version of the model giving a better account of the effects of molecular sizes is proposed below.

The pseudophase separation approach will be applied to aqueous micellar solutions of NaDS and C₁₂AO where the following chemical reactions occur (hereinafter we use the brief designation AOS for the complex):



The discussion below pertains to surfactant concentrations significantly above the cmc (the overall surfactant content is fixed, $x_{\text{total}} = 0.001$). In this region, the composition of mixed micelles is approximately equal to the overall surfactant-only based composition of the solution ($x'_{\text{AO}}, x'_{\text{NaDS}} = 1 - x'_{\text{AO}}$). The “true” equilibrium composition of the micellar system is described by the variables $z_i = \tilde{n}_i / (m_{\text{AO}} + m_{\text{NaDS}})$, where \tilde{n}_i ($i = \text{AOS}, \text{DS}^-, \text{AO}, \text{AOH}^+$) is the number of moles of the various species, and m_{AO} and m_{NaDS} are the overall numbers of moles of the surfactants. The activities of the species are estimated in the approximation of the athermal mixture of monomers (DS⁻, AO, AOH⁺) and dimers (AOS). Evidently, for the volume fraction of monomers we have $\varphi_i = z_i$, for the complex $\varphi_{\text{AOS}} = 2z_{\text{AOS}}$. According to the Flory equations,

$$\ln a_i = \ln \varphi_i + \varphi_{\text{AOS}}/2 \quad \text{where } i = \text{DS}^-, \text{AO}, \text{AOH}^+$$

$$\ln a_{\text{AOS}} = \ln \varphi_{\text{AOS}} - 1 + \varphi_{\text{AOS}} \quad (5)$$

The conditions of chemical equilibria can be written as

$$K_a' = \frac{\varphi_{\text{AOH}^+}}{\varphi_{\text{AO}} \times 10^{-\text{pH}}} \quad \text{and} \quad K_{\text{AOS}} = \frac{\varphi_{\text{AOS}}}{\varphi_{\text{DS}^-} \varphi_{\text{AOH}^+}} \quad (6)$$

where $K_a' = 1/K_a$ is the protonation constant.

The true composition can be found from these equations and the material balance constraints:

$$\begin{aligned} \varphi_{\text{AOS}}/2 + \varphi_{\text{AO}} + \varphi_{\text{AOH}^+} &= x'_{\text{AO}} \\ \varphi_{\text{AOS}}/2 + \varphi_{\text{DS}^-} &= 1 - x'_{\text{AO}} \end{aligned} \quad (7)$$

The following quadratic equation results from eqs 6 and 7:

$$\varphi_{\text{AOS}}^2/4 - \varphi_{\text{AOS}} \left[\frac{1}{2} + \frac{1}{K_{\text{AOS}}} \left(1 + \frac{1}{10^{-\text{pH}} K_a'} \right) \right] + x'_{\text{AO}} (1 - x'_{\text{AO}}) = 0 \quad (8)$$

Knowing the values of K_a' and K_{AOS} (which are assumed to be temperature independent), one can find the true concentrations of various species in a mixture of a given surfactant-based mole fraction x'_{AO} at fixed values of pH. These values of true concentrations are substituted into relationships describing the solubility curves.

For concentrated solutions of ionic surfactants, it is convenient to describe thermodynamic conditions of the micellar solution–solid surfactant equilibrium in terms of the composition variables of micelles such as in the case of nonionic surfactants, because the degree of counterion binding is close to unity.³⁵

The solubility diagram in the concentration range 0.0 ≤ x'_{AO} ≤ 0.5 is presented by two intersecting branches,

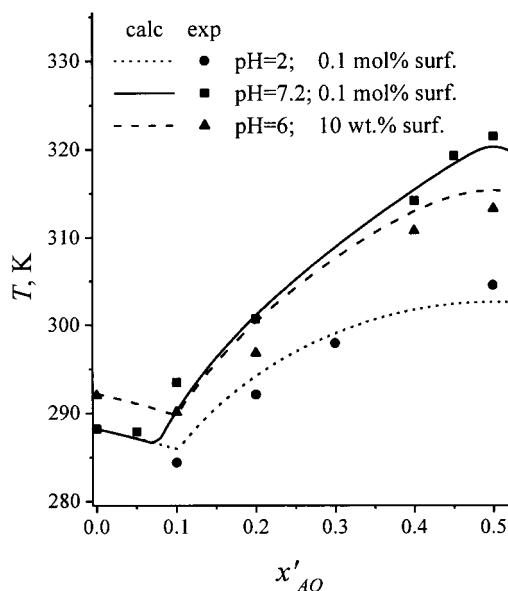


Figure 12. Dissolution curves in the $C_{12}AO-NaDS-H_2O$ system calculated by eqs 5–10 at a total surfactant content equal to 0.1 mol % (pH = 7.2 and pH = 2.0, $T_{NaDS}^0 = 288.2$ K) and 10 wt % (pH = 6, $T_{NaDS}^0 = 292.2$ K); $\Delta H_{NaDS} = 35$ kJ mol $^{-1}$, $\Delta H_{AOS} = 60$ kJ mol $^{-1}$, $T_{AOS}^0 = 321.4$ K, $K_{AOS} = 2.3 \times 10^3$. Points present experimental data.

which are the curves of crystallization of NaDS (its hydrate) and AOS. For the first curve, we can write

$$\ln a_{NaDS} = -\frac{\Delta H_{NaDS}}{R} \left[\frac{1}{T} - \frac{1}{T_{NaDS}^0} \right] \quad (9)$$

and for the second one,

$$\ln a_{AOS} = -\frac{\Delta H_{AOS}}{R} \left[\frac{1}{T} - \frac{1}{T_{AOS}^0} \right] \quad (10)$$

where T_i^0 is the dissolution temperature and ΔH_i is the differential molar enthalpy of dissolution of the pure component i ($i = NaDS, AOS$) at a given value of the overall surfactant content.

According to the literature and our data, for NaDS $\Delta H_{NaDS} = 35$ kJ/mol, and at $x_{total} = 0.001$ $T_{NaDS}^0 = 288.2$ K. The enthalpy of dissolution of the pure AOS complex was estimated from the experimental solubility diagram at pH = 2 by applying eq 10 and supposing that the entire amount of amine oxide enters the complex, which corre-

sponds to $\varphi_{AOS} = 2x'_{AO}$; $\ln a_{AOS} = \ln(2x'_{AO}) - 1 + 2x'_{AO}$. One gets $\Delta H_{AOS} = 60$ kJ/mol ($T_{AOS}^0 = 321.4$ K). The constant of the complex formation was adjusted to the data at pH = 7.2. The value giving a good fit of the results calculated by eqs 8–10 to the experimental dissolution diagram is $K_{AOS} = 2.3 \times 10^3$. For the protonation constant K'_a , the value 3.3×10^4 obtained from potentiometric titration experiments was taken (it agrees well with the value from ref 15). The procedure of a simultaneous adjustment of the enthalpy and the constant of complex formation gives values very close to that above. The estimated constant of complex formation relates to a concentrated micellar system and evidently differs from that for the reaction between monomer species in diluted aqueous solutions.

As is seen in Figure 12, the calculations reproduce general tendencies in location of the solubility curves in the aqueous mixture $C_{12}AO-NaDS$ at various pHs. The predicted dissolution curve at pH = 6 and a total surfactant content of 10 wt % is in satisfactory agreement with the experimental data.

Assuming the formation of the 1:1 complex, one can describe the solubility diagram in the range of mixing ratios $C_{12}AO/NaDS$ from 0:1 to 1:1. As for mixtures enriched with amine oxide where nonequimolar complexes can be formed, further experimental and theoretical studies would be of interest.

6. Conclusions

Strong synergistic effects are responsible for the specific phase behavior of amine oxide–sodium (magnesium) dodecyl sulfate micellar solutions.

The dissolution temperature and the cmc value are greatly dependent on the relative surfactant concentration and pH.

The phase diagrams in the two studied systems $C_{12}AO-MeDS-H_2O$ are quite similar at low pH and differ at the natural acidity.

At low pH, the complex AOH^+DS^- is crystallized over a wide range of surfactant-based concentrations.

The pH effect on the solubility diagrams of semipolar-anionic surfactant mixtures, not studied so far, was satisfactorily reproduced for the $C_{12}AO-NaDS-H_2O$ system by the proposed version of the pseudophase model considering the reactions of the amine oxide protonation and the 1:1 complex formation.

Acknowledgment. The authors highly appreciate the financial support of Procter & Gamble and the Russian Foundation for Basic Research (Project Nos. 00-15-97353 and 01-03-32319).

LA011508Y